Poultry Science®

Synergistic anti-infectious bronchitis virus activity of Phillygenin combined Baicalin by modulating respiratory microbiota and improving metabolic disorders

Haipeng Feng,* Jingyan Zhang,* Kang Zhang,* Xuezhi Wang,† Zhiting Guo,* Lei Wang,* and Jianxi Li*,[1]

*Engineering & Technology Research Center of Traditional Chinese Veterinary Medicine of Gansu Province, Lanzhou Institute of Husbandry and Pharmaceutical Sciences, Chinese Academy of Agricultural Sciences, Lanzhou, Gansu 730050, China; and †Lanzhou Veterinary Research Institute, Chinese Academy of Agricultural Sciences, Lanzhou, Gansu 730046, China

ABSTRACT Phillygenin (**PHI**) and Baicalin (**Bai**) are the major chemical ingredients extracted from *Forsythia suspensa* and *Scutellaria baicalensis*, respectively. The mixture of *Forsythia suspensa* and *Scutellaria baicalensis* according to the theories of Traditional Chinese Veterinary Medicine, compounded formulation can effectively exert heat-clearing and detoxifying effect, but the synergistic anti-IBV activity of PHI combined with Bai was unclear. Here, the protection of PHI combined with Bai on avian infectious bronchitis virus (**IBV**) M41 infection and the change of respiratory microbiota and metabolomics profiles in broilers that infected with IBV were investigated. According to the experimental findings, the combination of PHI and Bai effectively alleviated broilers' slowing-growth weight and respiratory symptoms. This was accompanied by a reduction in viral copies and histopathological changes, as well as an increase of antiviral protein (**G3BP1**) level in tracheas and anti-IBV antibody levels in serum. In addition, 16s RNA sequencing revealed that IBV infection significantly changed respiratory microbiota composition at different taxonomic levels and respiratory metabolism composition in broilers. Interestingly, PHI combined with Bai modulated the composition of respiratory microfloras, especially the abundance of *Firmicutes* and *Lactobacillaceae* were upregulated, as well as the abundance of *Proteobacteria* was downregulated. The metabolomics results indicated that PHI combined with Bai involved in glucose, lipids, amino acids and nucleotide metabolism during IBV infection. In summary, PHI combined with Bai exhibited a synergistic effect on preventing infectious bronchitis (**IB**), with the protection being closely associated with the composition of respiratory microbiota and metabolites. Therefore, adding the mixture of PHI and Bai to the chicken drinking water is recommended to prevent and control IB in clinical.

Key words: Respiratory microbiota, metabolite, Phillygenin, Baicalin, anti-IBV

2024 Poultry Science 103:103371

https://doi.org/10.1016/j.psj.2023.103371

INTRODUCTION

The poultry industry incurs significant economic losses due to respiratory infections, as avian infection through respiratory tract is a predominant mode of pathogen transmission. Avian infectious bronchitis virus (**IBV**) is one of the most severe viral respiratory pathogens that affecting birds, ranking second only to avian influenza and Newcastle disease. IBV, belongs to genus gamma coronavirus, is a positive sense, single-stranded nonsegmented RNA virus, about 27.6 kb in length (Cavanagh, 2003; Klestova et al., 2022). Birds are the natural host of IBV, with continuous mutation of virus and the emergence of new strains, live vaccines vaccination only provided partially protection efficacy due to the antigenic variation (Bayry et al., 2005; Yang et al., 2023a). Therefore, we should prioritize the development of anti-IBV drugs by leveraging the inherent advantages of traditional Chinese veterinary medicine, which exhibits a multicomponent and multitarget point in order to mitigate substantial economic losses.

The management of combination therapies for diseases has garnered significant attention. Baicalin (**Bai**), a flavonoid extracted from the root of *Scutellaria baicalensis Georgi*, is one of the most commonly and versatile herbal medicines used to antibacterial, antiviral, anti-inflammatory, protection liver and nerve in China. Previous literatures have reported that Bai have extensive antiviral effect in birds, such as NDV, MDV, ALV, DHAV-1 (Jia

Received September 14, 2023.

Accepted December 7, 2023.

[1]Corresponding author: lzjianxil@163.com

et al., 2016; Chen et al., 2018; Qian et al., 2018; Yang et al., 2020). Phillygenin (**PHI**) is a woody lipid active ingredient, mostly extracted from the Chinese herbal medicine *Forsythia suspensa*. PHI has many medicinal values, such as anti-inflammatory, antioxidant, anti-infection and immune regulation (Ma et al., 2023; Xue et al., 2023). Bai combined Berberine Hydrochloride, Bai combined emodin alleviated DSS-induced colitis in mouse by modulating gut microbiota and activating TLR4/NF-κB/PPAR-γ signaling pathway (Xu et al., 2021; Yan et al., 2022). The combination of Bai and EDTA as a novel colistin adjuvant can provide therapeutic measure for colistin resistant bacterial infection (Cui et al., 2023). Currently, there is a dearth of research on the synergistic antivirus activity of PHI combined Bai.

Previous results in our laboratory confirmed that PHI and Bai can inhibit IBV Beaudette strain replication in Vero cell, but their synergistic protective effect on broilers that infected with IBV M41 was unclear. Therefore, we hypothesized that the combination of PHI and Bai may exert a synergistic beneficial effect in preventing IBV infection by modulating respiratory microbiota and inducing metabolism changes. In this study, we explored 16S rRNA based micro-biological and untargeted metabolomics to investigate the change of respiratory microbiotas and metabolites after being treated with PHI combined Bai in IBV-infected broilers.

MATERIALS AND METHODS

Strain, Chemical Compounds, and Animals

The IBV M41 strain was purchased from the China Institute of Veterinary Drug Control and subsequently passaged blindly for 5 generations on specific pathogen-free (**SPF**) chicken embryos. The viral titer was determined using the Reed and Muench method, EID_{50} was found to be $10^{-5.78}$/0.1 mL (Reed and Muench, 1937). The drugs (PHI and Bai) were provided by Shaanxi Senfu Natural Products Co., Ltd. (Shaanxi, China) and has a purity of over 97% (HPLC $\geq$ 97%). One-day-old unimmunized male White Feather Broiler-type Commercial chicken weighing 40 $\pm$ 4 g were purchased from a local commercial hatchery (Jiuquan, Gansu, China). All procedures were carried out following guidelines by the Animal Care and Use Committee, Lanzhou Institute of Husbandry and Pharmaceutical Sciences of the Chinese Academy of Agricultural Sciences (the permission number : SYXK(Gan) 2019-0002).

Experimental Design

A total of 120 one-day-old white feather broilers were raised in a negative pressure isolator until they reached 7 d of age (**doa**). Subsequently, they were randomly divided into control group, IBV infected group, PHI + Bai group, and PHI + Bai + IBV group (30 birds per group). Broilers in PHI + Bai + IBV group were administrated with PHI and Bai mixture at a dose of 24 mg/mL and 450 mg/mL in the drinking water continuously for 7 d (Ishfaq et al., 2021; Guo et al., 2022). Then, except for the control group, other groups were challenged with IBV-M41 (10^4EID_{50}/0.1 mL per bird) 0.3 mL through an ocular-nasal route at 14 doa, and clinical signs were observed and recorded daily. Serum was collected from the heart at 14, 15, 17, and 19 doa for ELISA detection (8 birds per group). Then all broilers were humanized execution, and the upper end of about 2 cm trachea was fixed in neutral formalin solution for histopathology and immunohistochemistry observation, and the middle end of about 2 cm trachea was fixed in 2.5% glutaraldehyde solution for scanning electron microscope analysis, and the remaining was placed in a sterile centrifuge tube, which was frozen in liquid nitrogen and stored at -80°C for real-time quantitative PCR (**RT-qPCR**), 16sRNA and metabolomics analysis.

Hematoxylin and Eosin Staining and Immunohistochemical Test

Hematoxylin and eosin (**H&E**) staining was carried out to evaluate the degree of tracheal and lung injury. Briefly, tracheas and lungs were dissected and fixed immediately in 4% paraformaldehyde after birds were sacrificed humanely. Tissue samples that embedded in paraffin were cut into section of 5 μm thickness, and observed under a microscope after being stained with H&E.

Localization and distribution of IBV and G3BP1 in trachea was detected by immunohistochemical (**IHC**) assay. Trachea section that embedded was incubated with 3% hydrogen peroxide at room temperature (**RT**) for 25 min, then the samples were cultured with secondary antibody after being incubated with primary antibody. Finally, the distribution of proteins was observed after being stained with DAB, and performed quantitative analysis using image-J software.

Scanning Electron Microscope Analysis

The fixed tracheal tissue was fixed 1% osmic acid at RT darkly after being washed with phosphate buffer for 3 times. Then, the tissues were dehydrated in 30−50−70−80−90−95−100−100% ethanol and isoamyl acetate for 15 min, respectively. The sample was placed on the sample stage of the ion sputtering instrument for spraying gold for about 30 s after it was dried at critical point drying. Finally, it was observed under a microscope and taken pictures for analysis.

Specific Anti-IBV Antibody in Serum With ELISA Kit Detection

The commercial ELISA kit (Jiubang, Fujian, China) was recovered at RT when removing from 4°C. The antibody containing Streptavidin-**HRP** with 100 μL was added to each well and incubated under 37°C for 60 min after 50 μL samples and standards were added to each well, except for blank hole. The plate was washed with washing solution for 5 times and the plate that added

50 μL substrate A and B was incubated at 37°C in dark for 15 min. Finally, each well was added 50 μL stop solution and the optical density was detected at 450 nm, then the anti-IBV antibody concentration was calculated according to constructed standard curve.

Real-Time Quantitative PCR

Total RNA in tissues were extracted using Trizol reagent and was reverse- transcribed into cDNA using PrimeScript RT reagent kit with gDNA Eraser (Takara, Dalian, China) based on manufacturer's instruction. Absolute quantitative RT-PCR was used to quantify viral copies using SYBR Premix Ex Taq Ⅱ (Takara, Dalian, China). Cycle threshold (**CT**) value was converted to copies of viral RNA by generating a standard curve of six 10-fold dilutions of plasmid that was constructed in our laboratory. The mRNA expression of G3BP1 was standardized using CT value of β-actin. The sequence of primer was used as follows:

IBV (chicken): F-5'-GACGGAGGACCTGATGGTAA-3'
IBV (chicken): R-5'-CCCTTCTTCTGCTGATCCTG-3'
G3BP1 (chicken): F-5'-AGGGTGAACAAGGTGATGTGGAAAC-3'
G3BP1 (chicken): R-5'-GCCATAGCCTGCAAGAGAAGAGC-3'
β-actin (chicken): F-5'-CCCAAAGCCAACAGAGAGAA-3'
β-actin (chicken): R-5'-CCATCACCAGAGTCCATCAC-3'

Respiratory Microflora Analysis

Total DNA in sample was extracted using the OMEGA Soil DNA Kit (Omega Bio-Tek, Norcross, GA), following the manufacturer's instructions. The quantity and quality of extracted DNAs were measured using a NanoDrop NC2000 spectrophotometer. PCR amplification of the bacterial 16S rRNA genes V3 to V4 region was performed using the forward primer (F: 5'-ACTCCTACGGGAGGCAGCA-3') and the reverse primer (R: 5'-GGACTACHVGGGTWTCTAAT-3'). Sample-specific 7-bp barcodes were incorporated into the primers for multiplex sequencing. PCR amplicons were purified with Vazyme VAHTSTM DNA Clean Beads (Vazyme, Nanjing, China) and quantified using the Quant-iT PicoGreen dsDNA Assay Kit (Invitrogen, Carlsbad, CA). After the individual quantification step, amplicons were pooled in equal amounts, and pair-end 2 × 250 bp sequencing was performed using the Illumina MiSeq platform with MiSeq Reagent Kit v3 at Shanghai Personal Biotechnology Co., Ltd. (Shanghai, China). Microbiome bioinformatics were performed with QIIME2 2019.4 with slight modification according to the official tutorials (https://docs.qiime2.org/2019.4/tutorials/). Sequence data analysis was mainly performed using QIIME2 and R packages (v 3.2.0). Microbial functions were predicted by PICRUSt2 (Phylogenetic investigation of communities by reconstruction of unobserved states) upon MetaCyc (https://metacyc.org/) and KEGG (https://www. kegg.jp/) databases. The micro-flora in respiratory tract were finished by Shanghai Bioprofile Technology Co., Ltd. (Shanghai, China), detailed instruction exhibited in Supplemental Material 1.

Analysis of Metabolites in Respiratory Tract

Weighed Tracheal samples were ground in centrifuge tube containing a 5 mm tungsten bead for 1 min at 65 Hz in a Grinding Mill. Metabolites were extracted and then placed for 1 h ultrasonic shaking in ice baths. The supernatants were recovered and concentrated to dryness in vacuum after being centrifuged at 14,000 × g for 20 min at 4°C. Metabolomics profiling was analyzed using a UPLC-ESI-Q-Orbitrap-MS system (UHPLC, Shimadzu Nexera X2 LC-30AD, Shimadzu, Japan) coupled with Q-Exactive Plus (Thermo Scientific, San Jose). For liquid chromatography separation, samples were analyzed using a ACQUITY UPLC HSST3 column(2.1 × 100 mm, 1.8 μm) (Waters, Milford, MA). The electrospray ionization (**ESI**) with positive-mode and negative mode were applied for MS data acquisition separately. Quality control (**QC**) samples were prepared by pooling aliquots of all samples that were representative of the samples under analysis, and used for data normalization. The raw MS data were processed using MS-DIAL for peak alignment, retention time correction and peak area extraction. R (version: 4.0.3) and R packages were used for all multivariate data analyses and modeling. Data were mean-centered using Pareto scaling. The differential metabolite data were performed KEGG pathway analysis using KEGG database (http://www.kegg.jp). The metabolism analysis in respiratory tract was conducted by Shanghai Bioprofile Technology Co., Ltd. (Shanghai, China), detailed instruction exhibited in Supplemental Material 2.

Statistical Analysis

All bar plots in this study were formed with GraphPad Prism 9.0 (GraphPad Software, La Jolla, CA). An analysis of differential significance was performed by SPSS 26.0 (IBM SPSS, Chicago, IL) using a 1-way ANOVA test. For all comparisons, $P < 0.05$ was considered statistically significant, $P < 0.01$ was considered to be extremely significant.

RESULTS

Effects of PHI Combined Bai on Weight Growth and Clinical Signs in IBV-Infected Broilers

The body weight change of broilers in different groups throughout the entire experimental period are depicted in Supplemental Figure 1A. After being administrated with PHI + Bai compounds for 7 d, the difference in body weight growth between IBV and IBV + PHI + Bai group emerged. The weight growth speed in IBV + PHI + Bai group was

higher than that in IBV group, whereas body weight in PHI + Bai group was higher than other 3 groups. In addition, we found that broilers in IBV- infected group occurs feather erection, crowding, neck extension, wheezing, head shaking, and wing drooping occurs at 3 dpi and 5 dpi by recording the clinical signs daily. The broilers treated with the mixture of PHI and Bai only showed slight drooping wings at 5 dpi, while the control group had no clinical symptoms, as shown in Supplemental Figure 1B.

Effect of PHI Combined Bai on Pathological Change in IBV-Infected Broilers

H&E analysis showed that trachea and lung tissue structure was in normal form with perfect cell nucleus and cytoplasm in control group, but IBV infection caused the tracheal injury that mainly focused at 3 and 5 dpi. The pathological changes mainly contained gland hyperplasia in tracheal mucosal layer, cilia almost exfoliated, and a large number of lymphocytes and monocytes infiltration in the mucosal layer, accompanied by a small amount of bleeding in mucosal layer, whereas PHI combined Bai treatment reduced the damage severity, which only showed slight tracheal cilia exfoliation and mucosal hyperplasia at 5 dpi (Figure 1A). Scanning electron microscope (**SEM**) analysis further confirmed that PHI combined Bai alleviated the ultrastructure injury of trachea caused by IBV infection. In control group, the structure of tracheal mucosa was relatively normal, with scattered brush cells, the surface microvilli with dense structure and uniform thickness, cell membrane structure intact and tight junctions, widely distributed ciliary cells. In IBV group, the tracheal mucosa was injured severely, such as membrane damage and disintegration, the number of ciliated cells decreased, large areas of degeneration, most of which were significantly shorter and thinner, and a small number of goblet cell existed. In IBV + Bai + PHI group, the tracheal mucosa damage was relatively slight, which showed that brush cells slightly shrink and collapse, microvilli are sparse locally, the number of ciliated cells is slightly reduced, and goblet cell partially existed (Figure 2).

Histopathological observation confirmed that PHI combined Bai protect lung injury caused by IBV. Briefly, gross hemorrhaging in the parabronchus lumen emerged when broilers were challenged with IBV M41, especially at 3 dpi. However, only mild hemorrhaging in the parabronchus lumen occurred in IBV + PHI + Bai group at 5 dpi, and there was no significant pathological injury in control group (Figure 1B).

Effect of PHI Combined Bai on Anti-IBV Antibody Level in Serum

The anti-IBV antibody level in serum was detected by ELISA to further assess the effect of PHI-Bai compounds to immune response. The antibody levels exhibited a slow upregulation trend, peaked at 3 dpi and subsequently declined gradually. Notably, the antibody levels in IBV group were significantly lower compared to those observed in PHI + Bai + IBV group, as shown in Supplemental Figure 1C.

Effect of PHI Combined Bai on Viral Loads in Lung and Trachea

Viral loads in tissues is a typical indicator for evaluating the antiviral effect of drugs. In present study, RT-

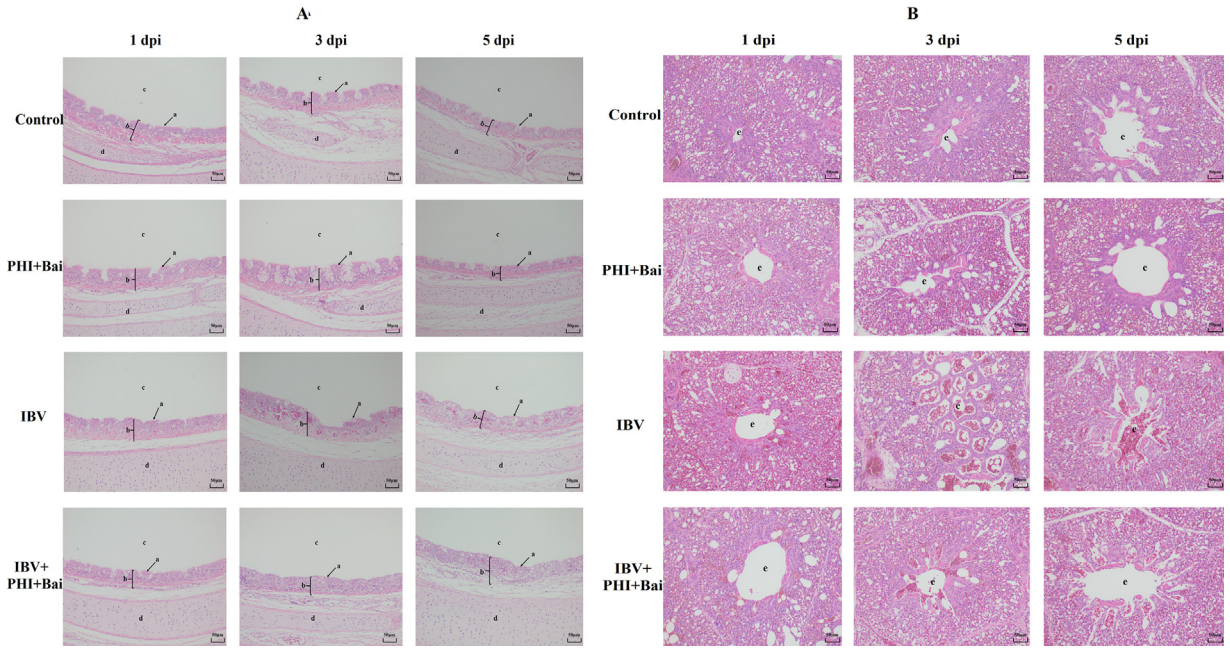

Figure 1. The histopathological changes in broilers. A represents tracheal (magnification, 200×), a indicates cilia; b indicates trachea mucosa; c indicates trachea lumen; d indicates trachea cartilage. B represents lung (magnification, 200×), e indicates parabroncheal lumen.

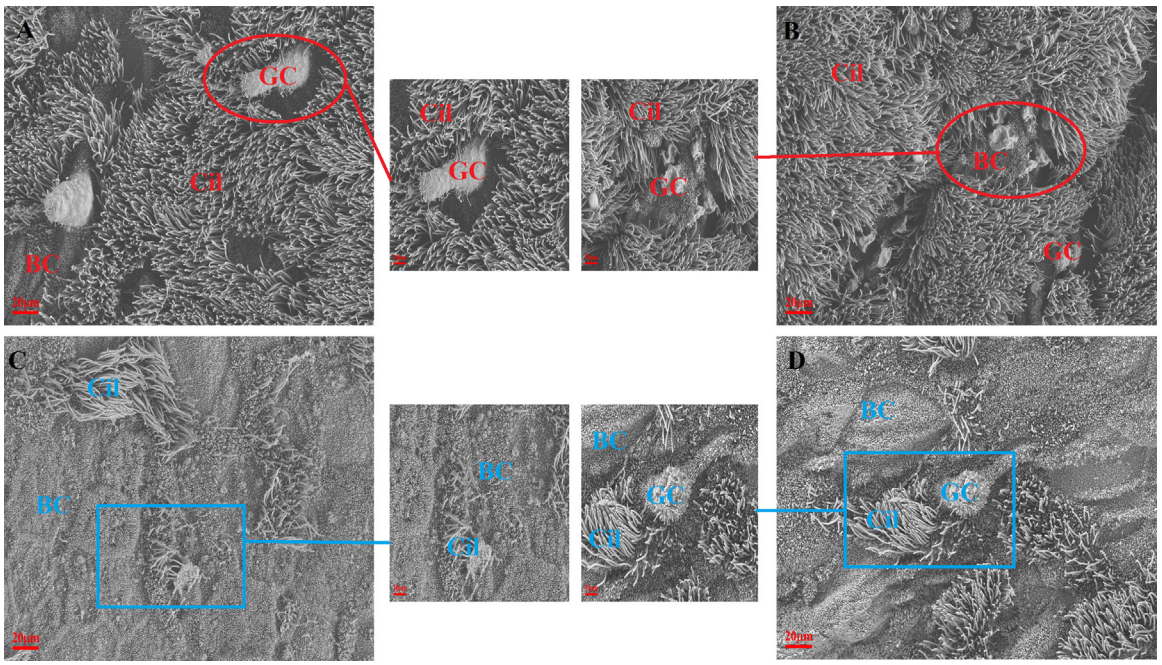

Figure 2. The ultrastructural change in broilers. A, B, C, and D represent the ultrastructural change of chicken trachea in control group, PHI + Bai group, IBV infected group, PHI + Bai + IBV group at a magnification of 2,500×, respectively. The red circle indicates that the cilia were more abundant and intact in both the control group and PHI treatment group at 5 dpi. The blue square demonstrates that the cilia were broken and shed in both the IBV infected group and PHI + Bai + group at 5 dpi. BC, CC, Cil, and GC indicate brush cells, ciliated cells, cilia and goblet cells in turn.

qPCR results demonstrated that IBV copies in the IBV + PHI + Bai group were declined compared to the IBV group during the experiment, especially there was significant difference in trachea and lung at 1 dpi and 5 dpi (Supplemental Figure 1D, E). The immunohistochemical localization analysis results indicated that IBV N protein was distributed in the tracheal mucosal surface and submucosal layer. There was no IBV distribution in control group, IBV N protein was mainly distributed in tracheal cartilage and mucosal surface in IBV group and IBV + PHI + Bai group, but the average of optical density (**AOD**) in IBV + PHI + Bai group was significantly higher than the IBV group during the experiment period ($P < 0.05$), as shown in Figure 3A.

Effect of PHI Combined Bai on G3BP1 Expression on Trachea

G3BP1, as an important antiviral protein, exerts a crucial role in blocking virus infection. The mRNA expression and distribution of G3BP1 in tracheal were evaluated, the results showed that the mRNA expression of G3BP1 in PHI + Bai + IBV group was higher than that in the IBV group at 3 and 5 dpi ($P < 0.05$), as shown in Supplemental Figure 2. The analysis of G3BP1 distribution in tracheal further confirmed PHI + Bai compound promoted the G3BP1 expression in tracheal during IBV infection, which manifested that G3BP1 was mainly distributed in the whole tracheal mucosa, and the AOD of G3BP1 exhibited consistent trend with the mRNA expression, as shown in Figure 3B, D.

Effect of Bai Combined PHI on α Diversity of Respiratory Microbial Community in Broilers

To further explore the anti-IBV mechanism of PHI-Bai compound, the respiratory floras were analyzed by 16s rRNA sequencing in tracheal bacterial DNA from different groups (normal, IBV, and IBV + PHI + Bai group). Firstly, to comprehensively evaluate the alpha diversity of microbial community, the Chao1 indices was used to characterize abundance, Shannon and Simpson indices was used to characterize diversity. The Venn chart that produced with ASV/OTU abundance table showed 556 OTUs were coexisted in respiratory microbiotas among all groups (Supplemental Figure 3B). The trend of rarefaction curves demonstrated that the curve of each group progressively flattened out with the increasing of sequencing volume, indicating that sequencing data were reasonable (Supplemental Figure 3A). Species accumulation curves and rarefaction curves for all samples to reflect the diversity and confirm the sampling effort's adequacy (Figure 4B). As shown in Figure 4C, IBV infection significantly decreased the Chao1 indices ($P < 0.01$). Although Shannon and Simpson indexes were increased in IBV group compared with normal group, there was no significant difference ($P > 0.01$), and there were no statistically significant differences in the Chao1, Shannon or Simpson indexes between IBV and IBV + PHI + Bai group. Furthermore, the rank abundance distribution curves reflect the number of high abundance and rare ASV/OTUs in the community, which revealed that increased abundance and relative bacterial imbalance between the IBV and IBV + PHI + Bai group compared to the normal group, as illustrated in Figure 4A.

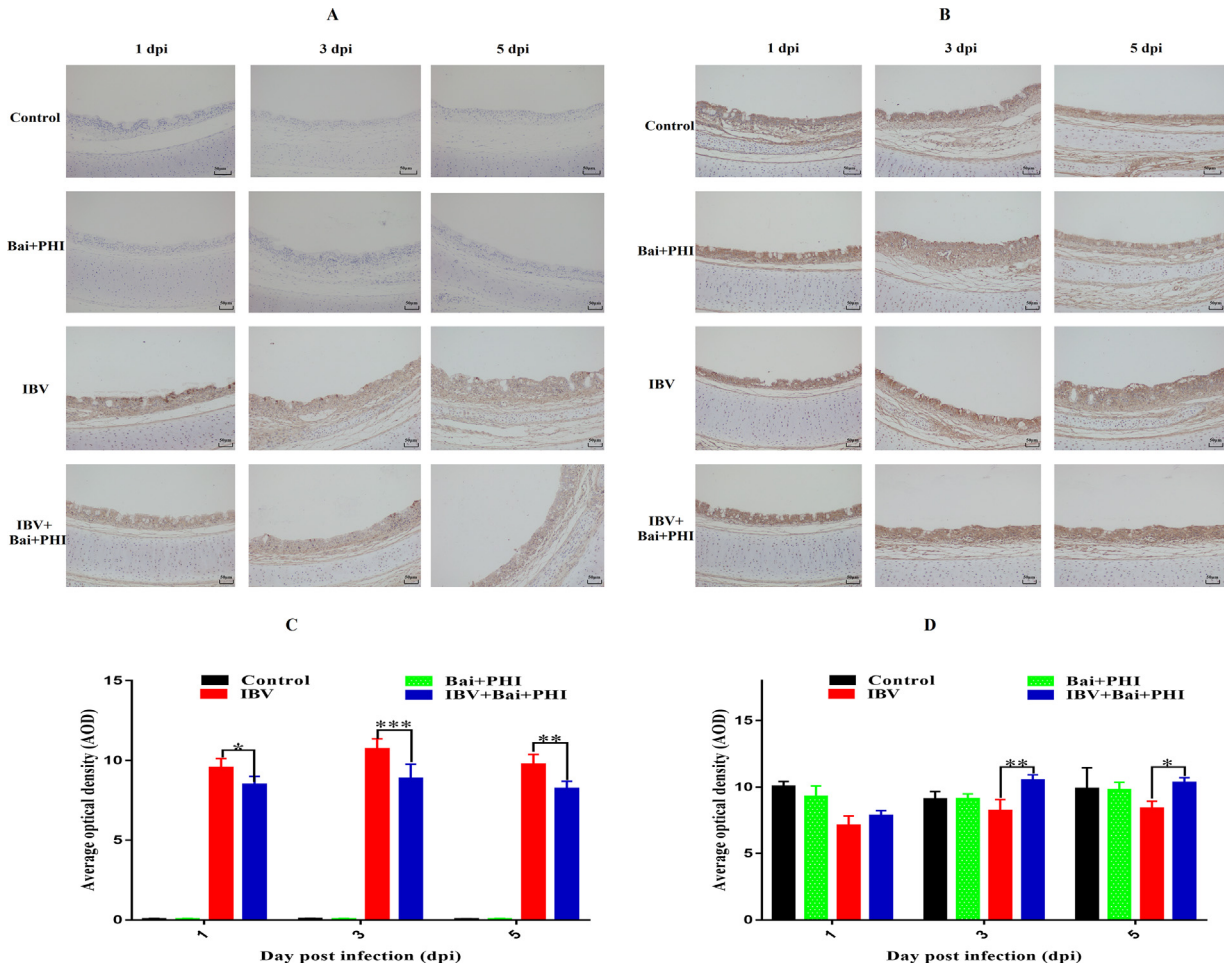

Figure 3. The distribution of IBV N protein and G3BP1 in tracheal. A, B represent IBV N and G3BP1, respectively. C, D indicated the visualization result of IBV N and G3BP1. Statistical significant are denoted by * $P < 0.05$, ** $P < 0.01$ and *** $P < 0.005$. These data were expressed as the mean ± SD, $N = 3$.

Effect of Bai Combined PHI on β Diversity of Respiratory Microbial Community in Broilers

Beta diversity reduces the dimensionality of multidimensional microbial data by means of unconstrained sorting methods, such as principal coordinate analysis (**PCoA**) and nonmetric multidimensional scaling (**NMDS**), which act the primary trends in data variation by distributing samples along continuous sorting axes. The similarity of community structure among all groups was compared using PCoA analysis based on Weighted Unifrac distance. The 2-dimensional PCoA result revealed distinct clustering of microbiota composition in different groups, with significant overlap between the control group and the IBV + PHI + Bai group, indicating a similar bacterial community structure (Supplemental Figure 4A). The NMDS results further confirmed the close proximity of each sample within their respective groups, indicating minimal differences in microbial communities among the groups (Supplemental Figure 4B). In this study, Wilcoxon test was performed to confirm top 20 significant alterations in tracheal microbial composition among the control group, IBV group and IBV + PHI + Bai group at phylum, family, genus level, respectively. As exhibited in Figure 5A, the relative abundance of *Coriobacteriaceae, Methylobacteriaceae* at the level of family was increased and the relative abundance of *Lactobacillaceae* was reduced in the IBV group compared the control group. Interestingly, the relative abundance of *Lactobacillaceae* was increased in IBV + PHI + Bai group and decreased the relative abundance of *Coriobacteriaceae, Methylobacteriaceae* compared the IBV group. At phylum level, PHI + Bai compound treatment reversed the reduction of *Firmicutes* abundance and the increasing of *Proteobacteria* abundance caused by IBV infection, as shown in Figure 5B. At genus level, IBV infection was characterized by an increase in *Methylobacterium* and lack of *Lactobacillus*, the opposite trend appears after being treated with PHI + Bai compound, as shown in Figure 5C.

Linear discriminant analysis effect size (**LEfSe**) was performed for pairwise comparisons among various groups to uncover biomarker. The more important an element was in the comparison, the higher the linear discriminant analysis (**LDA**) score based on the effect of bacterial genera in each group with a preset value of 4, and the lower the score, the less significant an element was. According to the LEfSe analysis of the respiratory

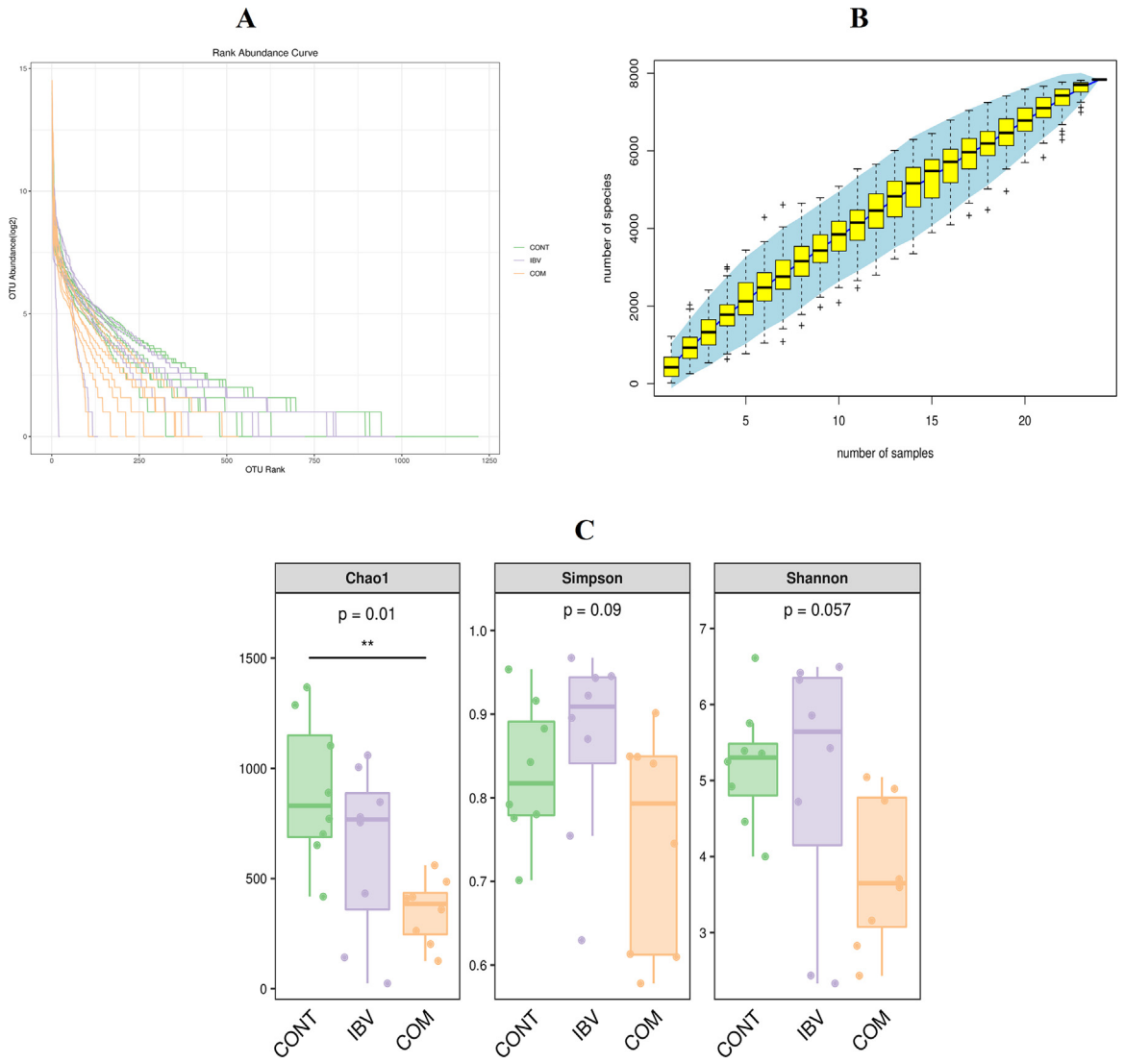

Figure 4. A represents the specaccum species accumulation curve. B represents abundance level curve. The smoothness of the broken line reflects the evenness of community composition. A flatter broken line indicates a smaller difference in abundance between each ASV/OTU in the community, thereby indicating higher evenness of community composition. Conversely, a steeper broken line suggests lower evenness. C represents the indices of Chao1, Shannon and Simpson.

microbial community, the change in relative abundance among 3 groups was caused by 17 species, with 4, 9, and 4 species in the normal, IBV, and IBV + PHI + Bai group, respectively (Figure 5D, E). These results indicated that IBV infection altered respiratory microbiota composition and population structure, and PHI + Bai compound improved the disorder of respiratory microbiota.

Effect of PHI Combined With Bai to Respiratory Tract Metabolites Regulation

Viral infection is closely associated with the host body's metabolism of amino acids, fatty acids, and nucleotides metabolism. Therefore, natural medicine may play a pivotal role in regulating respiratory metabolites to exert its antiviral effect. Principal component analysis (**PCA**) was conducted on the peaks extracted from all experimental and quality control sample after the data were standardized. QC samples exhibited a tight clustering in mixed positive and negative mode and the percentage changes in the first 2 PCA components were 15.04 and 12.13%, which indicated excellent experiment repeatability and trustworthy results (Figure 6A). Orthogonal partial least squares discriminant analysis (**OPLS-DA**) was used to find, screen and identify the differential metabolites with variable importance projection (**VIP**) ≥ 1 and $P < 0.05$. The results showed that R^2, $Q^2 \geq 0.5$, which indicated that the OPLS-DA model is stable and reliable, with good explanatory and predictive abilities (Figure 6B, C). The results of screening for differential metabolites are visualized in the form of volcanic diagrams and circular heat map, as illustrated in Figure 7. The scatter colors represent the final screening results, with 145 significantly upregulated metabolites denoted in red and 99 significantly downregulated metabolites indicated in green

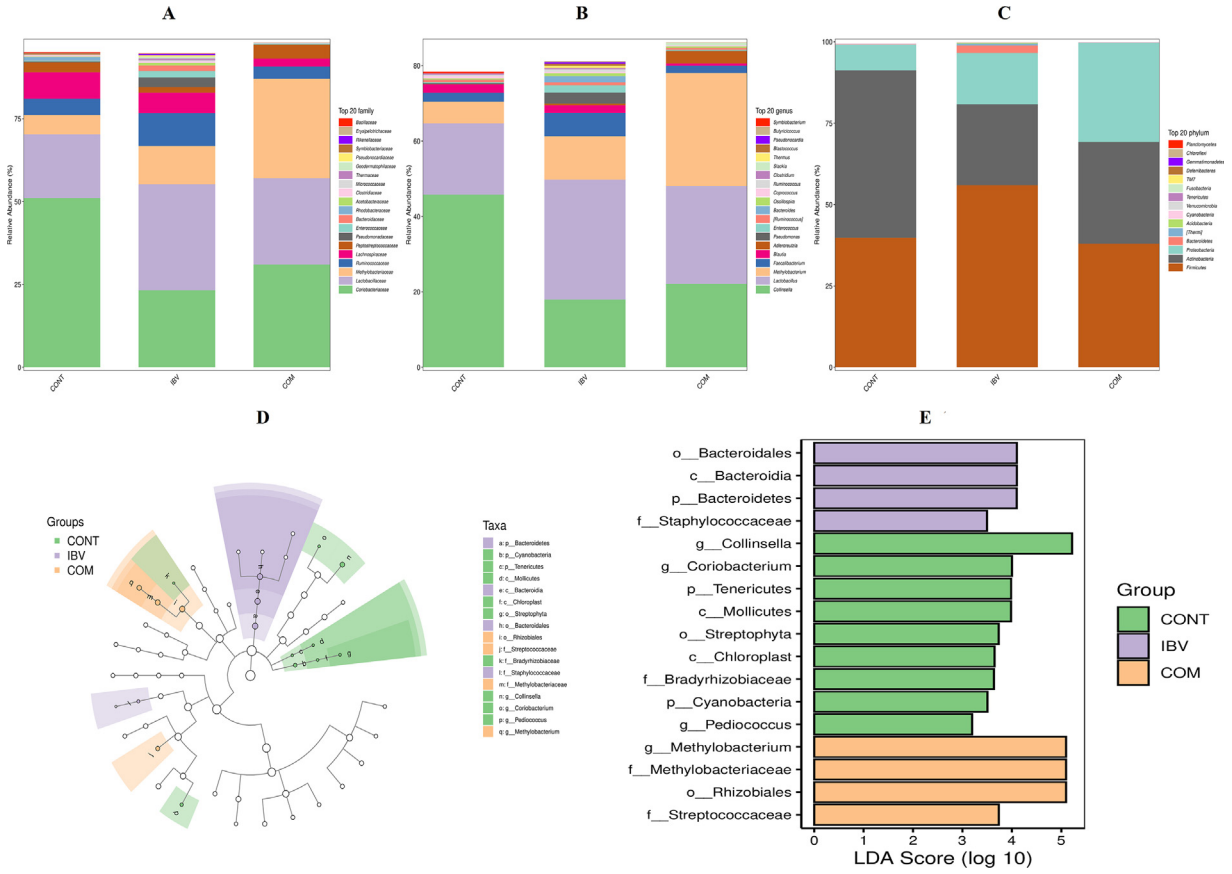

Figure 5. The abundance of respiratory tract floras. A, B, C indicated the relative abundance of the top 10 abundant bacteria at the phylum, family, and gene level. D represents the display diagram of inter group difference classification units. E indicated histogram of LDA effect values for marker species. LEfSe identified the abundance of cecal microbiota. The specific differential cecal microbial taxa that focused on each group were characterized with different colors.

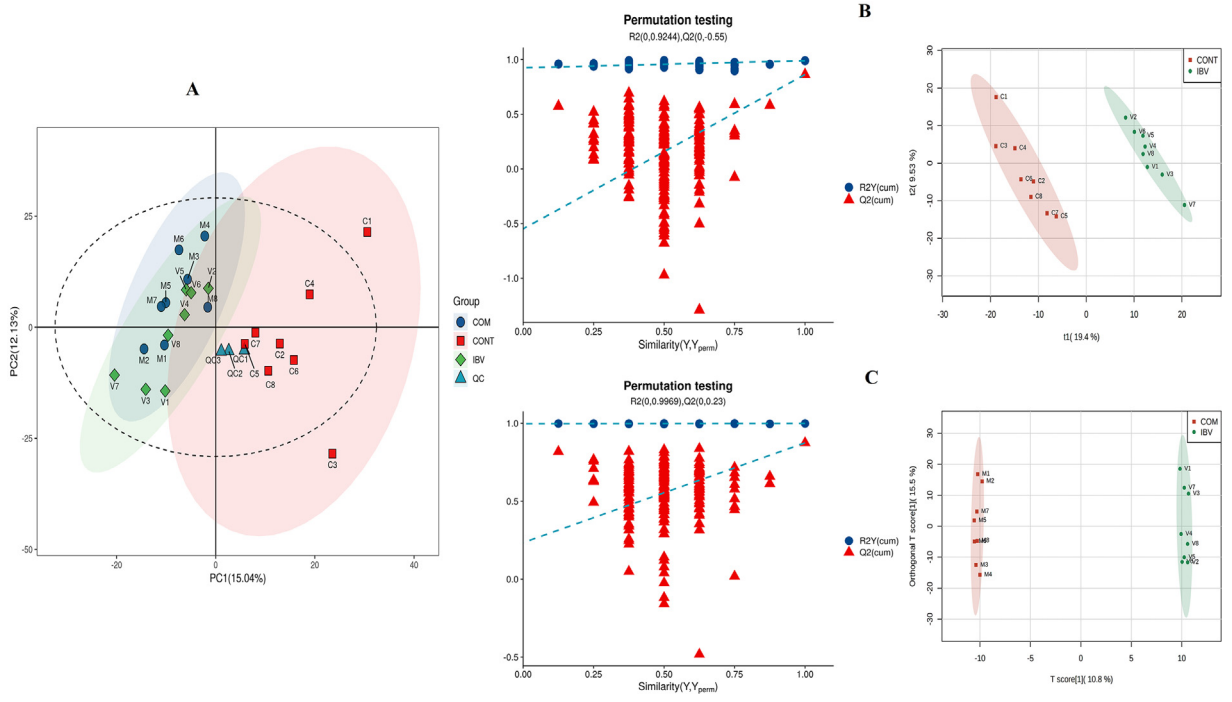

Figure 6. A represents PCA score chart. B represents PLS-DA permutation test chart and score chart between control and IBV group. C represents PLS-DA permutation test chart and score chart between IBV group and treatment group.

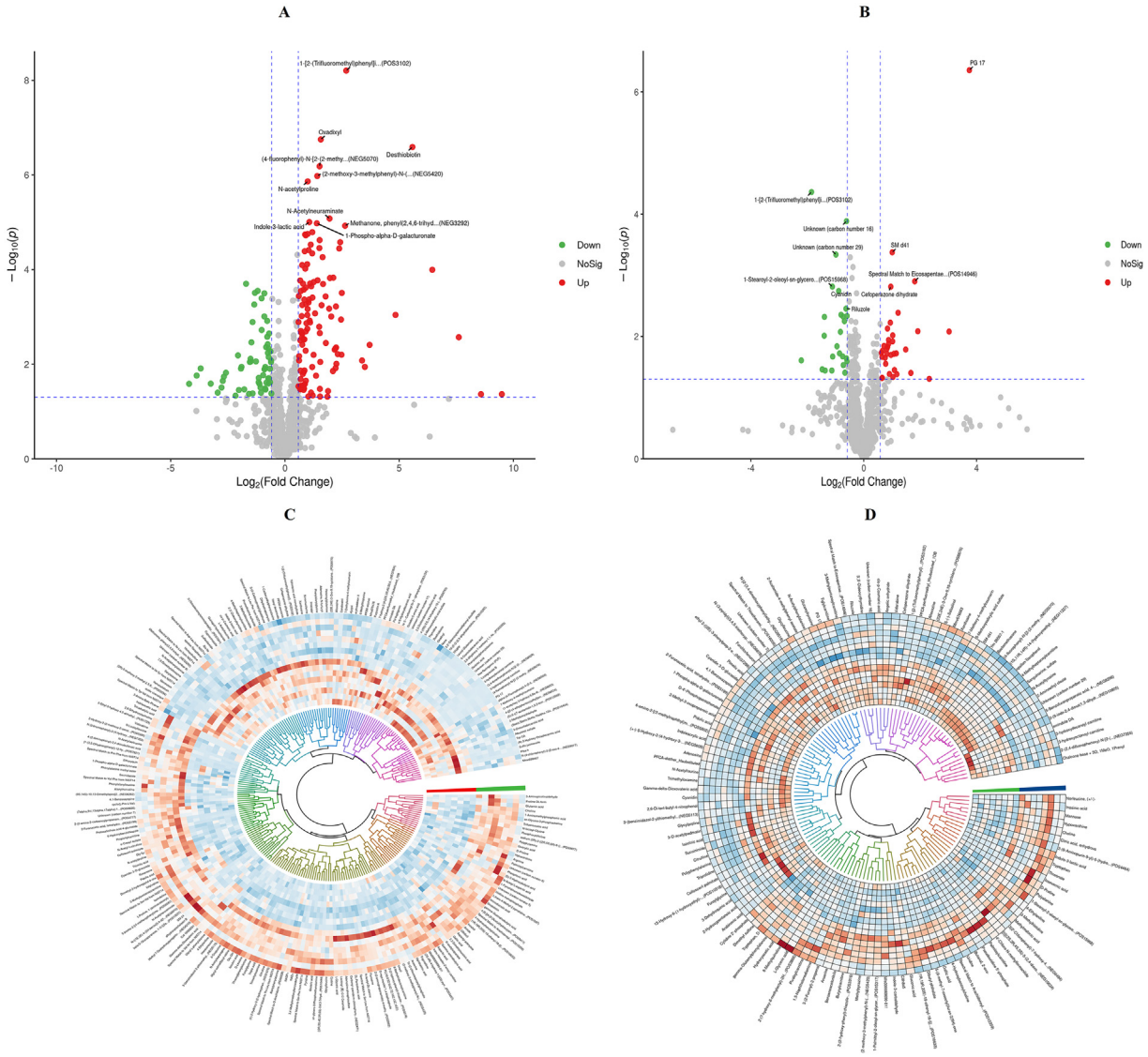

Figure 7. A, C represent the volcano map and circular heat map of differential metabolites between control and IBV group. B, D represent the volcano map and circular heat map of differential metabolites between IBV group and treatment group. The abscissa in the diagram represents the logarithm (base 2) of multiple changes within a group compared to between groups, while each point represents a metabolite. The ordinate represents the negative logarithm (base 10) of the P value obtained from Student t test. Each point in the diagram represents a metabolite and the abscissa represents multiple changes within a group in comparison to between group (the logarithm with 2 as the bottom), and the ordinate represents the P value of the Student t test (the negative number of the logarithm with 10 as the bottom). The scatter point size represents the VIP value of the OPLS-DA model.

between control and IBV group. Similarly, there were also 52 significantly upregulated metabolites denoted in red and 80 significantly downregulated metabolites indicated in green between the IBV and IBV + PHI + Bai group, while nonsignificantly different metabolites were shown in gray.

Effect of the Combination of PHI and Bai to Respiratory Tract Metabolic Pathway

Kyoto Encyclopedia of genes and genomes (**KEGG**) pathway analysis is the most direct and essential approach to systematically and comprehensively comprehend the biological processes of cells, traits or disease pathogenesis, drug action mechanisms. KEGG analysis help us to unveil the relationship between PHI + Bai compounds' function and metabolites in tracheal of broilers infected with IBV in our study. The KEGG analysis of differential metabolisms showed that ABC transporters, neuroactive ligand-receptor interaction, phosphatidylinositol signaling system, MTOR signaling pathway, aminoacyl-tRNA biosynthesis, arginine biosynthesis, alanine, aspartate and glutamate metabolism, nicotinate and nicotinamide metabolism, beta-alanine metabolism, biosynthesis of amino acids, biosynthesis of cofactors, purine metabolism, arginine and proline metabolism, glycerophospholipid metabolism, pyrimidine metabolism, glutathione metabolism, D-flutamine and D-glutamate metabolism, oxidative phosphorylation, histidine metabolism, nitrogen metabolism, drug metabolism—other enzymes, ether lipid metabolism, glyoxylate and dicarboxylate metabolism, pantothenate

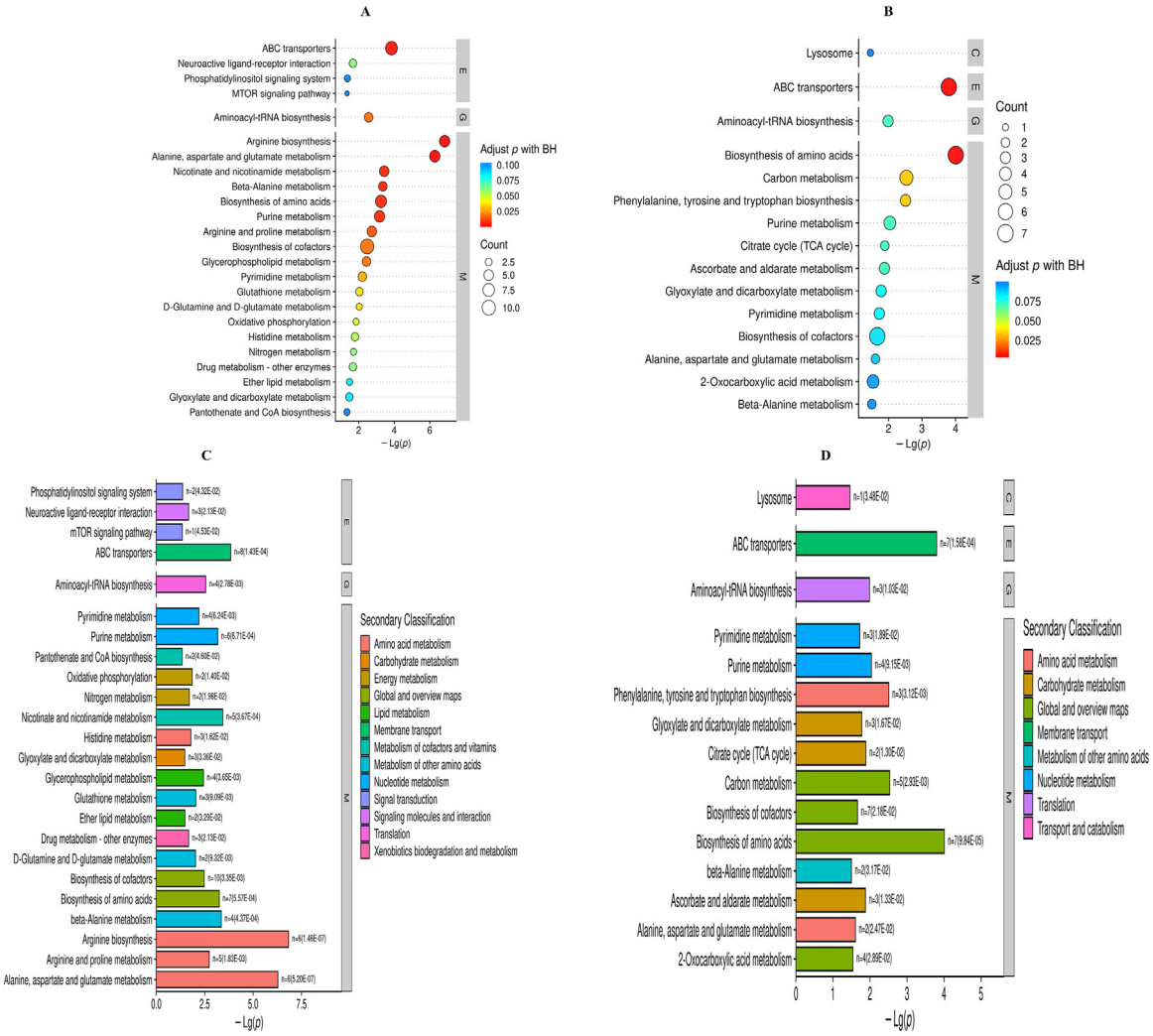

Figure 8. A, C represent KEGG pathway enrichment bubble chart (top 30) and bar chart of differential metabolites between control and IBV group. B, D represent KEGG pathway enrichment bubble chart (top 30) and bar chart of differential metabolites between IBV group and treatment group. The abscissa represented the negative logarithmic transformation of *P* value and the ordinate denoted pathway name. Pathways are categorized into KEGG level 1 group, ranked in descending order of significance based on −log10 (*P* value), indicating a sequential increase in *P* value and decrease in statistical significance. The size of the circle indicates the count, which represents the number of differential metabolites annotated into the pathway. The color of the circle corresponds to the corrected *P* value, with a gradient from red to blue indicating increasing significance.

and CoA biosynthesis were changed between IBV and control group (Figure 8A, C). Additionally, PHI + Bai treatment changed the pathway of lysome, ABC transporters, aminoacyl-tRNA biosynthesis, biosynthesis of amino acids, carbon metabolism, phenylalanine, tyrosine and tryptophan biosynthesis, purine metabolism, citrate cycle, ascorbate and aldarate metabolism, glyoxylate and dicarboxylate metabolism, pyrimidine metabolism, biosynthesis of cofactors, alanine, aspartate and glutamate metabolism, 2-oxocarboxylic acid metabolism, beta-alanine metabolism (Figure 8B, D).

DISCUSSION

This study represents the first investigation into the combination effect of PHI and Bai on respiratory tract microbiota and metabolic abnormality, and to identify the changes of respiratory microbiota and metabolites in IBV-infected broilers by using 16s rRNA-based microbiological and metabolomics analysis. There are increasing evidences indicated that the combined application of different natural products has exhibited outstanding advantages in the prevention and treatment of viral diseases (Xu et al., 2021; Shi et al., 2023). Additionally, the combined application has demonstrated to enhance therapeutic efficacy and expanding the range of targeted viruses compared to individual medication, and facilitate dosage reduction and minimizes drug toxicity. The combination of Osthole and Matrine had the synergistic effect of anti-PCV2 infection by directly inhibiting the expression of PCV2 Cap protein (Xu et al., 2020). In the present study, the combination of PHI with Bai effectively attenuated the slow-growth of body weight gain, reduced viral loads, alleviated tissue histopathological and ultrastructural injury, elevated anti-IBV antibody level, and upregulated the expression of G3BP1. Besides, microbiome and metabolomics data revealed that PHI

combined Bai improved respiratory microbiota disorders and changed the composition of tracheal metabolites. Overall, these results demonstrated that the mechanism of PHI combined Bai against IBV infection may be through regulating respiratory microbiota and its metabolites changes.

The rapid mutation of IBV and the poor-immune effect of vaccines resulted in significant economic losses in poultry health breeding. The clinical symptoms of IBV infection is associated with impaired weight gain in broilers and reduced efficiency of egg production in laying hens. The IBV-infected broilers model was constructed in this study, which presented the microscopic symptoms in broilers such as slow weight gain and respiratory tract disorder. After being pretreated with PHI and Bai compounds, IBV infection did not cause serious clinical symptoms or weight losses. These results confirmed that the combination of PHI with Bai could effectively reduce the economic losses in the breeding process of broiler. PHI and Bai compounds also exhibited excellent protective effect against IBV in broiler, as evidenced by viral loads, pathological, antibody levels, and G3BP1 expression. Our results indicated that PHI and Bai compounds alleviated tracheal pathological damage, reduced virus loads in tissues, promoted the anti-IBV antibody level and G3BP1 expression, which is also consistent with the antiviral effect of the majority of natural products. Previous research has demonstrated that *Olea europaea* leaves and propolis extracts mixture improved performance parameters of broiler chickens, alleviated microscopic lesions and viral shedding in tissues (Sawsan et al., 2023). The plant essential oils alleviated IBV-induced clinical signs, reduced viral loads, and upregulated antibody level in broiler (Zhang et al., 2022). G3BP1, as an important antiviral protein, play a crucial role in virus replication and immune response, making it a promising target protein for screening antiviral drugs (Zhao et al., 2022). Our research demonstrated that PHI and Bai compounds promoted the expression of G3BP1 in trachea, which illustrated that PHI and Bai compounds exerted a direct protect effect to IBV infection by upregulating G3BP1 expression. However, the formation mechanism of G3BP1 deserved to further explore by combining vitro and vivo experiments. Collectively, these findings indicated that PHI and Bai compounds may represent a promising and efficacious candidate drug to protect broiler against IBV infection, but the underlying mechanism remains unclear.

In general, a heightened diversity in microbial communities corresponds to a diminished likelihood of disrupting the delicate equilibrium of microorganisms, thereby facilitating to maintain a healthy internal environment for human body. For instance, an increased diversity of intestinal bacteria is associated with a reduced probability of developing conditions such as obesity and enteritis (Zhu et al., 2022; Wang et al., 2023). The microbial community reside in the upper respiratory tract exerts colonization resistance, effectively impeding pathogen colonization and thereby reducing the likelihood of lung infection (Vientós-Plotts et al., 2023). The disruption of the upper respiratory microbiota is associated with the pathogenesis of secondary infections that caused by respiratory virus. The virus infection is related with the diversity of upper respiratory microbiota alterations, and it is hypothesized that the increased proliferation rate of pathogenic bacteria constitutes a pivotal process in influenza virus infection (Li et al., 2023). Previous research have confirmed the effectiveness of probiotics in alleviating respiratory infection, thus providing a basis for investigating the underlying antiviral mechanism of natural product against respiratory viruses (Forsgård et al., 2023). Our results exhibited that IBV infection reduced relative abundance of *Lactobacillaceae* and *Firmicutes*, increased the abundance of *Proteobacteria, Coriobacteriaceae*, and *Methylobacteriaceae* in broilers' trachea. PHI and Bai compounds treatment upregulated the abundance of *Lactobacillaceae* and *Firmicutes*, and downregulated *Proteobacteri*a abundance. According to reported literatures, the *Lactobacillus* and *Firmicutes*, as beneficial bacteria, effectively establish a microbial barrier in the respiratory tract, thereby enhancing the barrier function of respiratory epithelial cells. The combination of *Lactobacillus acidophilus* and *Glycyrrhiza glabra* has demonstrated a potent inhibitory effect on the replication of HSV-1 and VSV, thereby exhibiting significant antiviral activity (Elebeedy et al., 2023). The concurrent administration of *lactobacillus* and *bacillus* probiotics during the rearing period effectively alleviated clinical and subclinical manifestations associated with H9N2 virus infection, thereby presenting a promising strategy for attenuating the severity of AIV H9N2 infection in broilers (Rasaei et al., 2023). In addition, certain *Proteobacteria* can also elicit detrimental effect on human and animal health, giving rise to respiratory, urinary tract, and gastrointestinal infection. The infection of ALV-J and NDV primarily resulted in an increased abundance of *Bacteroidetes* and *Proteobacteria*, consequently leading to significant alterations in the structure and composition of respiratory microbiota, which revealed that microbial community dysbiosis rendered broilers more susceptible to viral infection (Chen and Li, 2022; Tong et al., 2022). Findings from the current study that IBV infection in broilers caused alterations in the respiratory tract microbiota, and the maintenance of the host-microbial homeostasis within respiratory tract may represent one of the mechanisms by which PHI and Bai compounds exerted anti-IBV effect.

Metabolomics techniques become a powerful tool for determining metabolite changes and further analyzing the interaction between viruses and host. For instance, HBV infection regulates innate immunity by activating glycolysis, inhibiting retinoic acid-inducible gene I-induced interferon production (Zhou et al., 2021; Dai et al., 2022). SARS-CoV-2 infection hijacks the folate and carbon metabolism viral replication, and influences amino acid and fatty acid metabolism (Zhang et al., 2021). Zika virus infection reprograms the placental lipidome to support viral replication and provokes inflammation of the human placenta (Chen et al., 2020).

ASFV infection increased acylcarnitines level and inhibited the production and metabolism of acylcarnitines to block virus replication (Yang et al., 2023b). Recent studies confirmed that metabolomics has helped to widely understand various host responses during viral infection in chickens, such as the metabolomics of the kidney that infected IBV (Xu et al., 2019), bursa of Fabricius infected IBSV (Kuang et al., 2020), lungs that infected NDV (Liu et al., 2019), plasma that infected AIV-J (Chen et al., 2021) and chicken cell lines (DF-1 and LMH) that infected IBDV (Lin et al., 2020) were analyzed to clarified the mechanism in virus-host interactions. The metabolomics results in our study indicated that PHI and Bai compounds treatment showed a significant difference in lysome, ABC transporters, aminoacyl-tRNA biosynthesis, biosynthesis of amino acids, carbon metabolism, phenylalanine, tyrosine and tryptophan biosynthesis, purine metabolism, citrate cycle, ascorbate and aldarate metabolism, glyoxylate and dicarboxylate metabolism, pyrimidine metabolism, biosynthesis of cofactors, alanine, aspartate and glutamate metabolism, 2-oxocarboxylic acid metabolism, beta-alanine metabolism compared with IBV-infected group, which illustrated that PHI and Bai compounds regulated energy support during IBV replication. In summary, these metabolites changes increased the understanding to intracellular reactions which PHI and Bai compounds exerts anti-IBV effect by manipulating host's metabolic pathway. Accumulating evidence has indicated that cellular metabolism can be hijacked to facilitate viral replication. Cellular metabolites, metabolic regulators, and metabolic enzymes involved in cellular metabolism including glucose, lipids, amino acids and nucleotide metabolism, exert antiviral activities by regulating the host immune responses (Mirzaei et al., 2022). Previous studies have shown that infection with coronavirus (Rudiansyah et al., 2022), herpes virus (Gou et al., 2020), or African swine fever virus (Xue et al., 2022) can induce alternations in immune cell metabolism. Therefore, elucidating the effect of viruses on cellular metabolites, metabolism-related molecules and metabolic enzymes will facilitate the development of novel antiviral strategies (Boodhoo et al., 2020). These researches provided findings also verified in our study that PHI and Bai compounds protect broiler against IBV infection by manipulate host cellular metabolism during virus replication.

CONCLUSIONS

Taken together, the synergistic effect of PHI and Bai alleviated clinical symptoms and pathological changes caused by IBV infection, promoted G3BP1 expression and anti-IBV antibody level, and effectively protect broilers against IBV infection. In addition, PHI-Bai compounds treatment upregulated *Lactobacillaceae* and *Firmicutes* abundance, as well as downregulated *Proteobacteria* abundance in IBV-infected broilers. These results indicated the combination of PHI with Bai improved the respiratory tract floras disorder and involved in many energy metabolic pathways in IBV-infected broilers, which maybe a potential and effective drug compounds for preventing IB in poultry industry.

ACKNOWLEDGMENTS

This work was supported by the Agricultural Sciences and Technology Innovation Program (grant number CAAS-ZDXT2018008 and CAAS-LMY-02), the National Natural Science Foundation of China (No. 32202848).

DISCLOSURES

The authors declare that there was no conflict of interest.

SUPPLEMENTARY MATERIALS

Supplementary material associated with this article can be found in the online version at doi:10.1016/j.psj.2023.103371.

REFERENCES

Bayry, J., M. S. Goudar, P. K. Nighot, S. G. Kshirsagar, B. S. Ladman, J. Gelb, G. R. Ghalsasi, and G. N. Kolte. 2005. Emergence of a nephropathogenic avian infectious bronchitis virus with a novel genotype in India. J. Clin. Microbiol. 43:916–918.

Boodhoo, N., N. Kamble, S. Sharif, and S. Behboudi. 2020. Glutaminolysis and glycolysis are essential for optimal replication of Marek's disease virus. J. Virol. 94:31.

Cavanagh, D. 2003. Severe acute respiratory syndrome vaccine development: experiences of vaccination against avian infectious bronchitis coronavirus. Avian Pathol. 32:567–582.

Chen, Q., J. Gouilly, Y. J. Ferrat, A. Espino, Q. Glaziou, G. Cartron, R. Al-Daccak, and N. Jabrane-Ferrat. 2020. Metabolic reprogramming by Zika virus provokes inflammation in human placenta. Nat. Commun. 11:2967.

Chen, Y., and H. Li. 2022. Avian leukosis virus subgroup J infection influences the gut microbiota composition in Huiyang bearded chickens. Lett. Appl. Microbiol. 74:344–353.

Chen, Y., H. W. Li, F. Cong, and Y. X. Lian. 2021. Metabolomics profiling for identification of potential biomarkers in chickens infected with avian leukosis virus subgroup J (ALV-J). Res. Vet. Sci. 139:166–171.

Chen, Y., W. Yuan, Y. Yang, F. Yao, K. Ming, and J. Liu. 2018. Inhibition mechanisms of Bai and its phospholipid complex against DHAV-1 replication. Poult. Sci. 97:3816–3825.

Cui, X. D., J. K. Zhang, Y. W. Sun, F. B. Yan, J. F. Zhao, D. D. He, Y. S. Pan, L. Yuan, Y. J. Zhai, and G. Z. Hu. 2023. Synergistic antibacterial activity of Bai and EDTA in combination with colistin against colistin-resistant Salmonella. Poult. Sci. 102:102346.

Dai, J., H. Wang, Y. Liao, L. Tan, Y. Sun, C. Song, W. Liu, C. Ding, T. Luo, and X. Qiu. 2022. Non-targeted metabolomic analysis of chicken kidneys in response to coronavirus IBV infection under stress induced by dexamethasone. Front. Cell Infect. Microbiol. 12:945865.

Elebeedy, D., A. Ghanem, S. H. Aly, M. A. Ali, A. H. I Faraag, M. K El-Ashrey, A. M Salem, M. A. E Hassab, and A. I. A. E. Maksoud. 2023. Synergistic antiviral activity of Lactobacillus acidophilus and Glycyrrhiza glabra against herpes simplex-1 virus (HSV-1) and vesicular stomatitis virus (VSV): experimental and in silico insights. BMC Microbiol. 23:173.

Forsgård, R. A., J. Rode, K. Lobenius-Palmér, A. Kamm, S. Patil, M. G. J. Tacken, M. A. H. Lentjes, J. Axelsson, G. Grompone, S. Montgomery, and R. J. Brummer. 2023. Limosilactobacillus reuteri DSM 17938 supplementation and SARS-CoV-2 specific

antibody response in healthy adults: a randomized, triple-blinded, placebo-controlled trial. Gut Microbes 15:2229938.

Gou, H., Z. Bian, Y. Li, R. Cai, Z. Jiang, S. Song, K. Zhang, P. Chu, D. Yang, and C. Li. 2020. Metabolomics exploration of pseudorabies virus reprogramming metabolic profiles of PK-15 cells to enhance viral replication. Front. Cell Infect. Microbiol. 10:599087.

Guo, J., W. R. Yan, J. K. Tang, X. Jin, H. H. Xue, T. Wang, L. W. Zhang, Q. Y. Sun, and Z. X. Liang. 2022. Dietary phillygenin supplementation ameliorates aflatoxin B1-induced oxidative stress, inflammation, and apoptosis in chicken liver. Ecotoxicol. Environ. Saf. 236:113481.

Ishfaq, M., Z. Wu, J. Wang, R. Li, C. Chen, and J. Li. 2021. Baicalin alleviates Mycoplasma gallisepticum-induced oxidative stress and inflammation via modulating NLRP3 inflammasome-autophagy pathway. Int. Immunopharmacol. 101:108250.

Jia, Y., R. Xu, Y. Hu, T. Zhu, T. Ma, H. Wu, and L. Hu. 2016. Anti-NDV activity of Bai from a traditional Chinese medicine in vitro. J. Vet. Med. Sci. 78:819–824.

Klestova, Z. S., A. K. Voronina, A. Y. Yushchenko, O. S. Vatlitsova, G. V. Dorozinsky, Y. V. Ushenin, V. P. Maslov, T. P. Doroshenko, and S. A. Kravchenko. 2022. Aspects of "antigen-antibody" interaction of chicken infectious bronchitis virus determined by surface plasmon resonance. Spectrochim Acta A Mol. Biomol. Spectrosc. 264:120236.

Kuang, J., P. Xu, Y. Shi, Y. Yang, P. Liu, S. Chen, C. Zhou, G. Li, Y. Zhuang, R. Hu, G. Hu, and X. Guo. 2020. Nephropathogenic infectious bronchitis virus infection altered the metabolome profile and immune function of the bursa of Fabricius in chicken. Front. Vet. Sci. 7:628270.

Li, H., X. Wu, H. Zeng, B. Chang, Y. Cui, J. Zhang, R. Wang, and T. Ding. 2023. Unique microbial landscape in the human oropharynx during different types of acute respiratory tract infections. Microbiome 11:157.

Lin, J., X. Yi, and Y. Zhuang. 2020. Coupling metabolomics analysis and DOE optimization strategy towards enhanced IBDV production by chicken embryo fibroblast DF-1 cells. J. Biotechnol. 307:114–124.

Liu, P., Y. Yin, Y. Gong, X. Qiu, Y. Sun, L. Tan, C. Song, W. Liu, Y. Liao, C. Meng, and C. Ding. 2019. In vitro and in vivo metabolomic profiling after infection with virulent Newcastle disease virus. Viruses 11:18.

Ma, C., C. Wang, Y. Zhang, Y. Li, K. Fu, L. Gong, H. Zhou, and Y. Li. 2023. Phillygenin inhibited M1 macrophage polarization and reduced hepatic stellate cell activation by inhibiting macrophage exosomal miR-125b-5p. Biomed. Pharmacother. 159:114264.

Mirzaei, R., N. Sabokroo, Y. Ahmadyousefi, H. Motamedi, and S. Karampoor. 2022. Immunometabolism in biofilm infection: lessons from cancer. Mol. Med. 28:10.

Qian, K., Z. R. Kong, J. Zhang, X. W. Cheng, Z. Y. Wu, C. X. Gu, H. X. Shao, and A. J. Qin. 2018. Bai is an inhibitor of subgroup J avian leukosis virus infection. Virus Res. 248:63–70.

Rasaei, D., S. A. Hosseinian, K. Asasi, S. S. Shekarforoush, and A. Khodakaram-Tafti. 2023. The beneficial effects of spraying of probiotic Bacillus and Lactobacillus bacteria on broiler chickens experimentally infected with avian influenza virus H9N2. Poult. Sci. 102:102669.

Reed, L. J., and H. Muench. 1937. A simple method of estimating fifty per cent endpoints. Am. J. Epidemiol. 27:493–497.

Rudiansyah, M., S. A. Jasim, Pour. Z. G. Mohammad, S. S. Athar, A. S. Jeda, R. I. Doewes, A. T. Jalil, D. O. Bokov, Y. F. Mustafa, M. Noroozbeygi, S. Karampoor, and R. Mirzaei. 2022. Coronavirus disease 2019 (COVID-19) update: from metabolic reprogramming to immunometabolism. J. Med. Virol. 94:4611–4627.

Sawsan, S. E., B. Hatem, O. N. Mai, A. Amira, H. Haitham, and E. Mohamed. 2023. Efficacy of Olea europaea leaves and propolis extracts in the control of experimentally induced infectious bronchitis in broiler chickens. German J. Vet. Res. https://api.semanticscholar.org/CorpusID:257820961.

Shi, H., X. Li, C. Hou, L. Chen, Y. Zhang, and J. Li. 2023. Effects of pomegranate peel polyphenols combined with inulin on gut microbiota and serum metabolites of high-fat-induced obesity rats. J. Agric. Food Chem. 71:5733–5744.

Tong, L., W. Wang, S. Ren, J. Wang, J. Wang, Y. Qu, A. F. E. Addoma, Z. Li, and X. Gao. 2022. The 16S rRNA gene sequencing of gut microbiota in chickens infected with different virulent Newcastle disease virus strains. Animals (Basel) 12:24.

Vientós-Plotts, A. I., A. C. Ericsson, and C. R. Reinero. 2023. The respiratory microbiota and its impact on health and disease in dogs and cats: a one health perspective. J. Vet. Intern. Med. 37:1641–1655.

Wang, D., Y. Deng, L. Zhao, K. Wang, D. Wu, Z. Hu, and X. Liu. 2023. GABA and fermented litchi juice enriched with GABA promote the beneficial effects in ameliorating obesity by regulating the gut microbiota in HFD-induced mice. Food Funct. 14:8170–8185.

Xu, B., S. Huang, Y. Chen, Q. Wang, S. Luo, Y. Li, X. Wang, J. Chen, X. Luo, and L. Zhou. 2021. Synergistic effect of combined treatment with Bai and emodin on DSS-induced colitis in mouse. Phytother. Res. 35:5708–5719.

Xu, P., P. Liu, C. Zhou, Y. Shi, Q. Wu, Y. Yang, G. Li, G. Hu, and X. Guo. 2019. A multi-omics study of chicken infected by nephropathogenic infectious bronchitis virus. Viruses 11:16.

Xu, Y., P. Sun, S. Wan, J. Guo, X. Zheng, Y. Sun, K. Fan, W. Yin, N. Sun, and H. Li. 2020. The combined usage of Matrine and Osthole inhibited endoplasmic reticulum apoptosis induced by PCV2. BMC Microbiol. 20:303.

Xue, H. H., J. J. Li, S. F. Li, J. Guo, R. P. Yan, T. G. Chen, X. H. Shi, J. D. Wang, and L. W. Zhang. 2023. Phillygenin attenuated colon inflammation and improved intestinal mucosal barrier in DSS-induced colitis mice via TLR4/Src mediated MAPK and NF-κB signaling pathways. Int. J. Mol. Sci. 24:23.

Xue, Q., H. Liu, Z. Zhu, F. Yang, Y. Song, Z. Li, Z. Xue, W. Cao, X. Liu, and H. Zheng. 2022. African swine fever virus regulates host energy and amino acid metabolism to promote viral replication. J. Virol. 96:e0191921.

Yan, Y., L. Li, K. Wu, G. Zhang, L. Peng, Y. Liang, and Z. Wang. 2022. A combination of Bai and Berberine hydrochloride ameliorates dextran sulfate sodium-induced colitis by modulating colon gut microbiota. J. Med. Food 25:853–862.

Yang, X., X. Bie, H. Liu, X. Shi, D. Zhang, D. Zhao, Y. Hao, J. Yang, W. Yan, G. Chen, L. Chen, Z. Zhu, F. Yang, X. Ma, X. Liu, H. Zheng, and K. Zhang. 2023b. Metabolomic analysis of pig spleen reveals African swine fever virus infection increased acylcarnitine levels to facilitate viral replication. J. Virol. 15:e0058623.

Yang, F., C. Feng, Y. Yao, A. Qin, H. Shao, and K. Qian. 2020. Antiviral effect of Bai on Marek's disease virus in CEF cells. BMC Vet. Res. 16:371.

Yang, C. Y., P. Peng, X. Liu, Y. Cao, and Y. Zhang. 2023a. Effect of monovalent and bivalent live attenuated vaccines against QX-like IBV infection in young chickens. Poult. Sci. 102:102501.

Zhang, Y., R. Guo, S. H. Kim, H. Shah, S. Zhang, J. H. Liang, Y. Fang, M. Gentili, C. N. O. Leary, S. J. Elledge, D. T. Hung, V. K. Mootha, and B. E. Gewurz. 2021. SARS-CoV-2 hijacks folate and one-carbon metabolism for viral replication. Nat. Commun. 12:1676.

Zhang, Y., X. Y. Li, B. S. Zhang, L. N. Ren, Y. P. Lu, J. W. Tang, D. Lv, L. Yong, L. T. Lin, Z. X. Lin, Q. Mo, and M. L. Mo. 2022. In vivo antiviral effect of plant essential oils against avian infectious bronchitis virus. BMC Vet. Res. 18:90.

Zhao, J., D. Feng, Y. Zhao, M. Huang, X. Zhang, and G. Zhang. 2022. Role of stress granules in suppressing viral replication by the infectious bronchitis virus endoribonuclease. J. Virol. 96:e0068622.

Zhou, L., R. He, P. Fang, M. Li, H. Yu, Q. Wang, Y. Yu, F. Wang, Y. Zhang, A. Chen, N. Peng, Y. Lin, R. Zhang, M. Trilling, R. Broering, M. Lu, Y. Zhu, and S. Liu. 2021. Hepatitis B virus rigs the cellular metabolome to avoid innate immune recognition. Nat. Commun. 12:98.

Zhu, T., B. Hu, C. Ye, H. Hu, M. Yin, Z. Zhang, S. Li, Y. Liu, and H. Liu. 2022. Bletilla striata oligosaccharides improve ulcerative colitis by regulating gut microbiota and intestinal metabolites in dextran sulfate sodium-induced mice. Front. Pharmacol. 13:867525.